ISSN 1061-8309, Russian Journal of Nondestructive Testing, 2013, Vol. 49, No. 4, pp. 196–205. © Pleiades Publishing, Ltd., 2013.
Original Russian Text © A.V. Belonosov, O.A. Chikova, V.V. Yurovskikh, D.S. Chezganov, 2013, published in Defektoskopiya, 2013, Vol. 49, No. 4, pp. 17–28.

ACOUSTIC METHODS

Examining the Structure of Mill Rolls Made of 9X2MΦ and 8X3CΓΦ Steels Using the Ultrasonic Method for Quality Control

A. V. Belonosov[a], O. A. Chikova[b], V. V. Yurovskikh[a], and D. S. Chezganov[c]

[a] *Uralmashzavod, Yekaterinburg, Russia*

[b] *Ural Federal University, Yekaterinburg, Russia*

[c] *Institute of Physics and Applied Mathematics, Institute of Natural Science, Ural Federal University, Yekaterinburg, Russia*

e-mail: A. Belonosov@uralmash.ru, chik63@mail.ru, valerik@k66.ru,dmit.chezganov@gmail.com

Received August 16, 2012

Abstract—The microstructure of specimens of 9X2MΦ and 8X3CΓΦ steels taken from working rolls of a reversing mill was examined. A correlation between characteristics of the crystal structure of the metal and the intensified attenuation of ultrasonic waves was found. Ultrasonic inspection was carried out using an ultrasonic flaw detector (Krautkramer Co.). The microstructure was examined by means of traditional metallographic analysis methods, which were implemented using a scanning electron microscope; X-ray spectral microanalysis and electron backscatter diffraction were used. The morphology and elemental composition of discontinuity flaws were studied; as well, phase maps, crystallite misorientation histograms, and Taylor factor maps were plotted for specimens taken from the defect zone of a 9X2MΦ steel working roll.

Keywords: ultrasonic inspection, discontinuity flaws, microstructure, ultrasound scattering, X-ray spectral microanalysis, texture analysis, Taylor factor, low-carbon complex alloy steel

DOI: 10.1134/S1061830913040025

INTRODUCTION

The ultrasonic inspection of working rolls of a reversing cold-rolling mill is aimed at the identification of defects in a metal, including internal discontinuity flaws. It is known that the absolute value of the ultrasound reflection coefficient at the boundary of a defect filled with a gas or air is close to unity. For a defect filled with slag, this coefficient is substantially lower; thin oxide films yield a weak reflected signal [1]. In ultrasonic-inspection practice, only a comparison of the signal produced by a defect with the signal yielded by an artificial reflector in a reference specimen is carried out, due to the impossibility of estimating the real size of a discontinuity flaw. In this case, the inspection sensitivity is fairly low and corresponds, as a rule, to an equivalent defect size of ∅5 mm.

According to OST 24.023.33–86, the presence of discontinuity flaws with an equivalent diameter of less than 7 mm is permissible. The ultrasonic inspection of working rolls of a reversing mill made of 9X2MΦ and 8X3CΓΦ steels at the Uralmashzavod has found zones of discontinuity flaws with a reflection power that is equivalent to ∅2–4 mm; in places, no bottom signal is recorded. This is a contestable fact for drawing a conclusion on the compliance of roll quality with the requirements of OST 24.023.33–86.

The issue of the correlation of the ultrasound speed in metals and alloys with their structural state, structural defects, stresses, and mechanical properties is still topical. It is known, for example, that the presence of nonmetal inclusions and carbide network in steels affects the acoustic characteristics of steel articles, but no dependence of the ultrasound speed on the structure is found; this makes judgment about the nature of the relationship between the acoustic characteristics and structure difficult [2–4].

Production practice shows that the presence of these defects is the main cause of faults in rolls from a reversing mill. Figure 1 shows the fracture diagram of a 8X3CΓΦ steel roll that failed after the rolling of over 19000 t of metal during a half year of operation. The barrel of the roll was disintegrated into a few pieces; fracturing was accompanied by local delaminations of the working layer. The middle part of the barrel ~ 800–900 mm long was disintegrated along the central axis into two pieces. Two nuclei were found

Fig. 1. The fracture diagram of the roll.

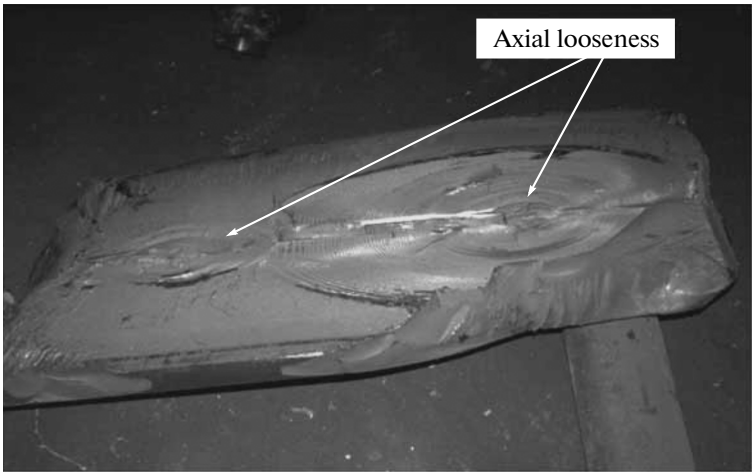

Fig. 2. An image of fracture nuclei of the roll.

in the longitudinal fracture of the barrel and fatigue fracture zones propagate from these nuclei (Fig. 2). The fracture of the roll shows zones with coarse-grained and fine-grained structures.

The type of the fracture nuclei of the roll (Fig. 2) is indicative of the presence of a dendritic or slaty fracture [5]. The cause of these types of fracture is an increased concentration of nonmetal inclusions that are arranged as strips after rolling. In steel articles, nonmetal inclusions such as oxides, sulfides, and silicates occur when a refractory material enters a liquid metal or agglomerates of deoxidizing products. This type of fracture (Fig. 2) can easily be confused with the fibrous structure that is intentionally formed in steels that are used to produce spring plates or springs by additional alloying with manganese and silicon.

The occurrence of cracks can be attributed to the presence of low-melting Fe–FeO–FeS eutectic that is located along grain boundaries. This effect is usually called hot brittleness; it is observed in steels with low concentrations of manganese and carbon. The cause is increased concentrations of oxygen and sulfur. Oxygen reduces the malting temperature of Fe–FeO–FeS eutectic [5].

Specimens were taken from the roll fracture zone and their microstructure was examined. Qualitative metallographic analysis has shown the presence of nonmetal inclusions: the granularity is four points for sulfides and five points for complex oxides according to GOST 1778–70 in the fatigue fracture zone in samples taken from the specimen core. The etching of the specimens has revealed the structure of lamellar and globular pearlite with a granularity of 2–4 points according to GOST 8233–56 in samples taken from the core. It is noted that the structure of the core metal is inhomogeneous due to the presence of lamellar and globular pearlite with various granularities [6]. Thus, in the core of the roll barrels, axial looseness occurs that is the nucleus of the origination and propagation of cracks. The roll metal has a brittle structure due to the presence of carbides arranged as a network that is located along grain boundaries (Fig. 3). The presence of nonmetal inclusions favored the origination and expansion of fatigue fracture zones that propagated from the core to the surface of the roll, thus resulting in roll fracture.

In addition, rolls made of 9X2MΦ and 8X3CΓΦ steels are frequently rejected at a producer factory according to the results of ultrasonic inspection. Inspection results are often controversial and require supplementary substantiation. For example, ultrasonic inspection has revealed a zone of discontinuity flaws along the full length of the barrel of a working roll made of the 9X2MΦ steel; it is permissible according

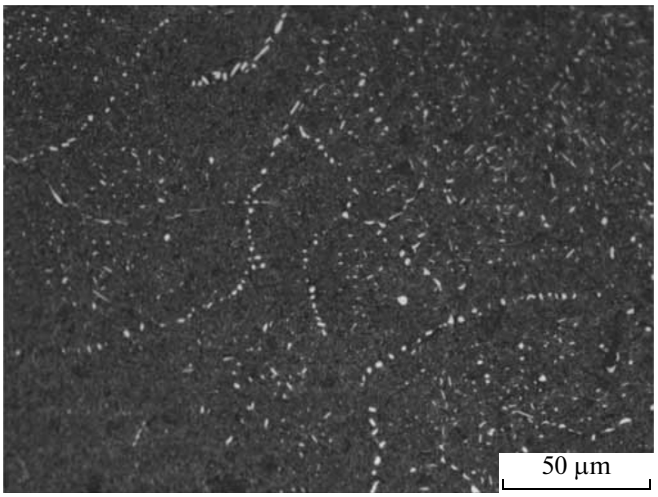

Fig. 3. The carbide network located along grain boundaries.

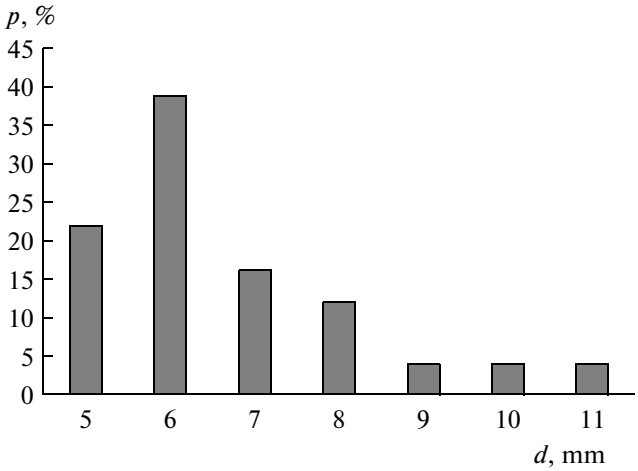

Fig. 4. The size distribution of discontinuity flaws.

to OST 24.023.33–86 and has an equivalent diameter of ∅4.5 mm and an occurrence depth of 120–350 mm. Numerous discontinuity flaws with a marginal size were also found in this zone (Fig. 4).

The aim of this work is to study the correlation between characteristics of the crystal structure of the metal, the presence of nonmetal inclusions less than 1 mm in size, and the intensified attenuation of ultrasonic waves in order to substantiate quality criteria for working rolls.

MATERIALS AND METHODS

The object of the study is samples taken from a 9X2MΦ steel roll. The chemical composition of the 9X2MΦ steel includes 0.01–0.02% of vanadium, 0.25–0.50% of silicon, 0.2–0.3% of molybdenum, 0.2–0.7% of manganese, 1.7–2.1% of chromium, and no more than 0.03% of sulfur. Working rolls are fabricated from 9X2MΦ steel forged pieces. The ultrasonic quality inspection of these rolls is carried out at the Uralmashzavod using a USM 35XS portable ultrasonic flaw detector (Krautkramer Co.); a coarse-grained structure, as well as inadmissible discontinuity flaws and other defects such as cracks are detected. I-20 industrial oil is used as a contact fluid for inspection. The USM 35XS flaw detector is equipped with two piezoelectric transducers with a resonance frequency of 2 MHz; these transducers induce oscillations in an article that are parallel and perpendicular to the wave vector. In accordance with the regulations, inspection implies the identification of transverse discontinuity flaws using an inclined transducer and

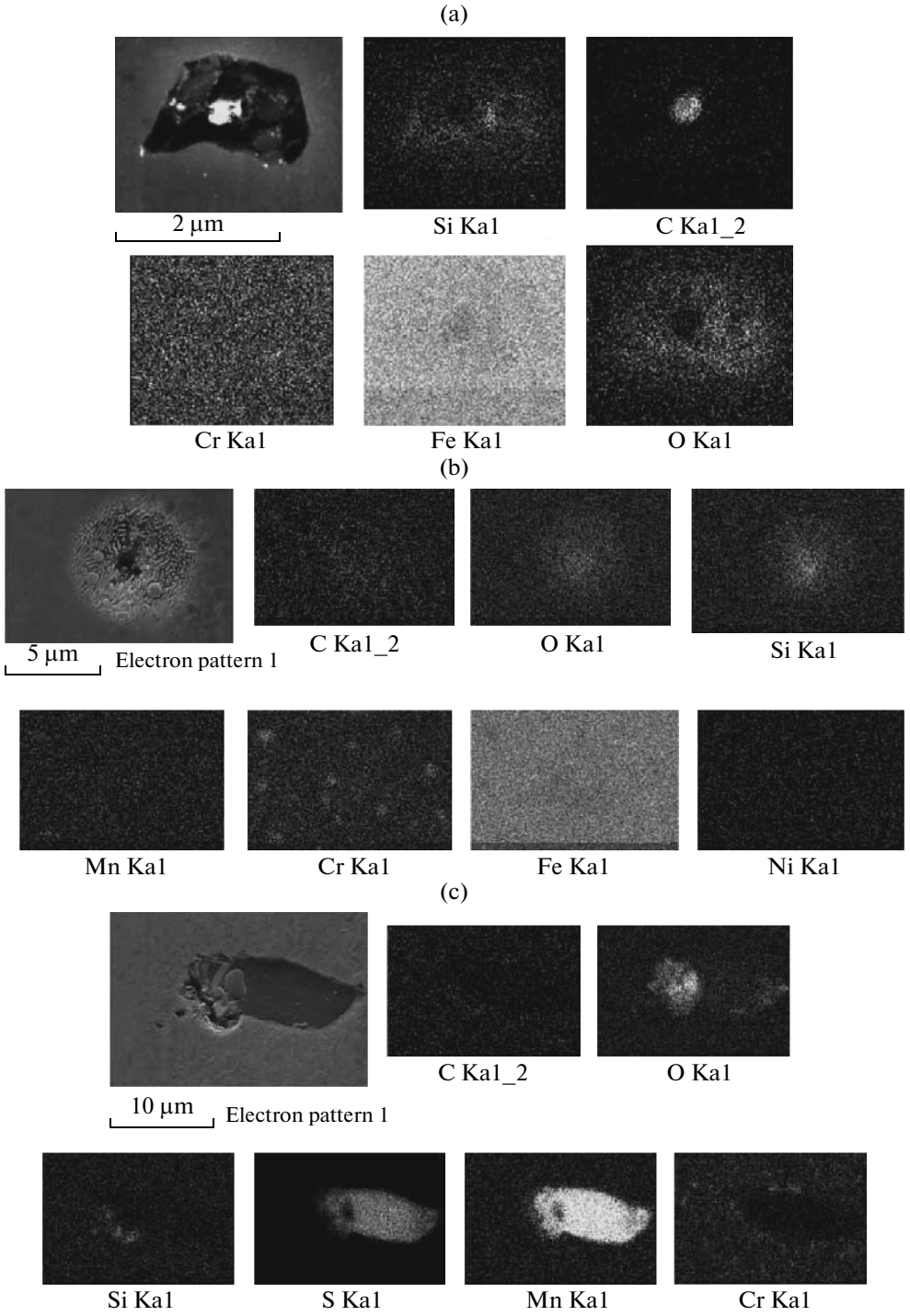

Fig. 5. The element distribution maps for (a) first-type, (b) second-type, and (c) third type inclusions.

defects using a perpendicular transducer. The inspection sensitivity is defined as an equivalent diameter of a discontinuity flow of 5 mm. Attenuation is not regulated, although this parameter is strictly regulated by international quality control standards.

In one of the rolls, a zone was found that contained an agglomerate of discontinuity flaws whose reflection power was equivalent to ∅2–4 mm; in places, no bottom signal was recorded. The ultrasonic inspection data was contestable for drawing a conclusion on the quality of the article and an additional study of the causes of the intensified ultrasound attenuation was required. A transverse macrotemplate was cut

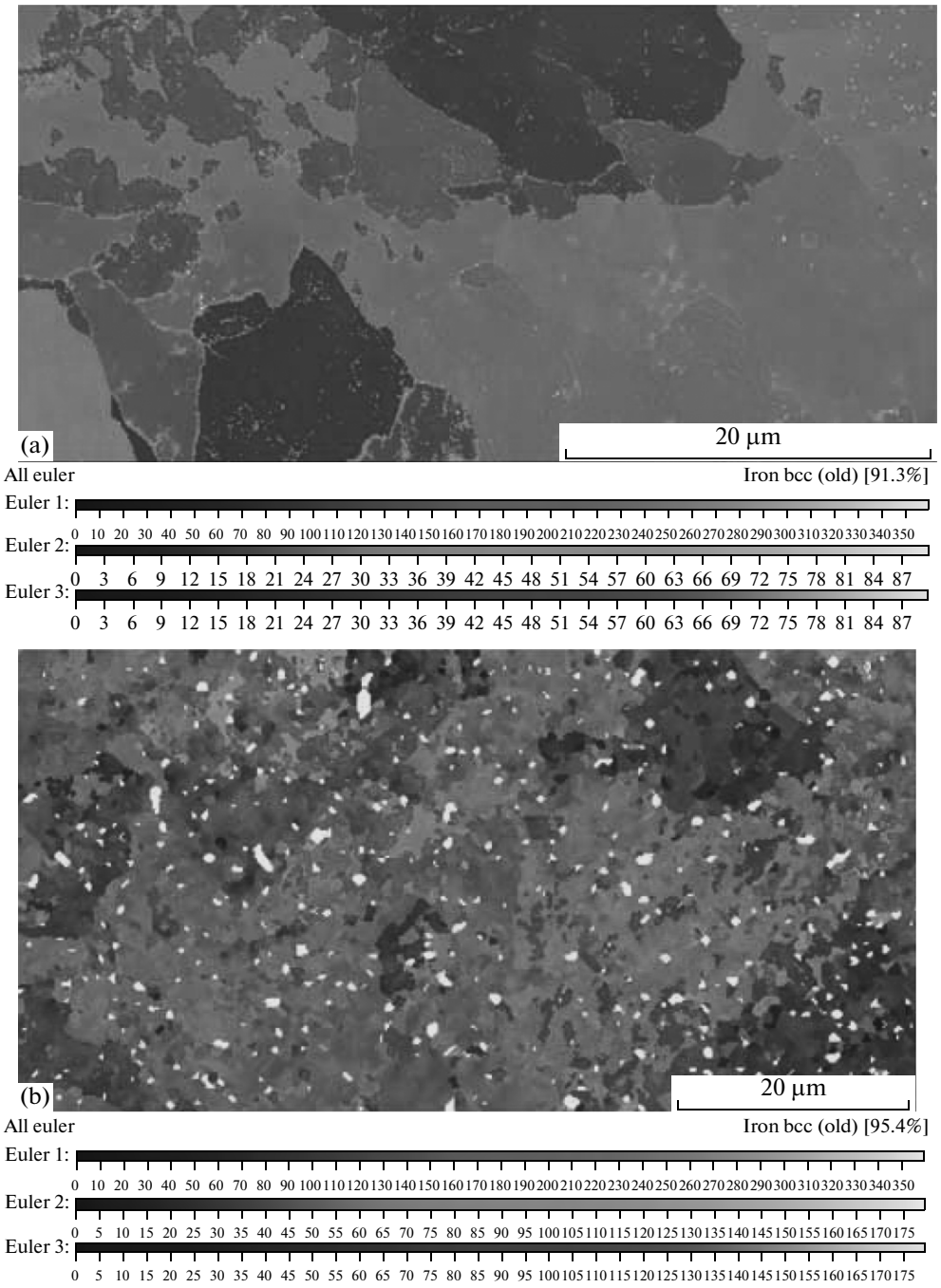

Fig. 6. The crystallite orientation map: (a) coarse crystallites and (b) fine crystallites.

from the roll barrel and samples that satisfied the data on the ultrasonic inspection of the defect zone were taken from this template. It was important to elucidate which specific features of the microstructure of working rolls of the mill made of the 9Х2МФ steel are responsible for the above-mentioned characteristics of the attenuation of ultrasonic oscillations during quality inspection.

It was assumed that the presence of nonmetal inclusions and an anisomerous structure with pronounced texture can affect the acoustic properties of the roll, thus producing additional sources for the scattering of ultrasonic oscillations and reducing the amplitude of the reflected signal obtained.

In order to verify this hypothesis we carried out a metallographic study of the metal structure using scanning electron microscopy [6]. The structure of specimens was examined by means of traditional metallography methods using an Auriga CrossBeam workstation. The Auriga CrossBeam workstation is a

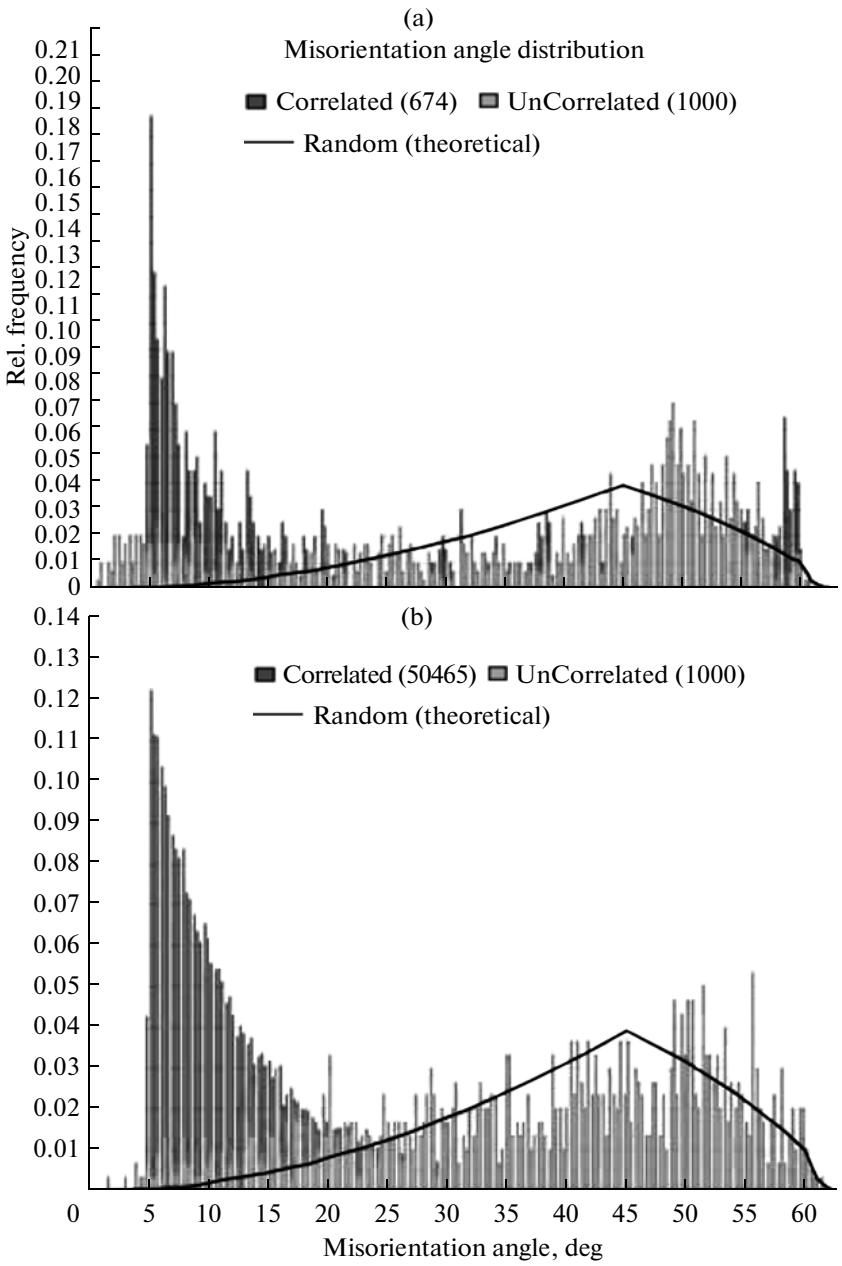

Fig. 7. The misorientation angle histogram for (a) coarse and (b) fine crystallites.

scanning electron microscope that is intended for studying the morphology, as well as the chemical and structural properties, of materials; it has a nanometer spatial resolution. In addition, a focused ion beam was used for sample preparation, energy-dispersive spectroscopy was applied for identifying the elemental composition of inclusions, and electron backscatter diffraction was involved for studying the crystal structure of the metal taken from the defect zone. The etching conditions for the surface of specimens used for texture analysis were as follows: 30 kV, 16 nA, and $\tau = 2$ min. This study was carried out in the Nondestructive Testing Laboratory of Uralmashzavod and in the Modern Nanotechnologies Center of Collaborative Access at the Institute of Natural Science of the Ural Federal University.

RESULTS AND DISCUSSION

Figures 5–9 show results of the metallographic study of the structure of specimens that were taken from a working roll of a mill made of the 9X2MΦ steel. Metallographic study was carried out by means of scan-

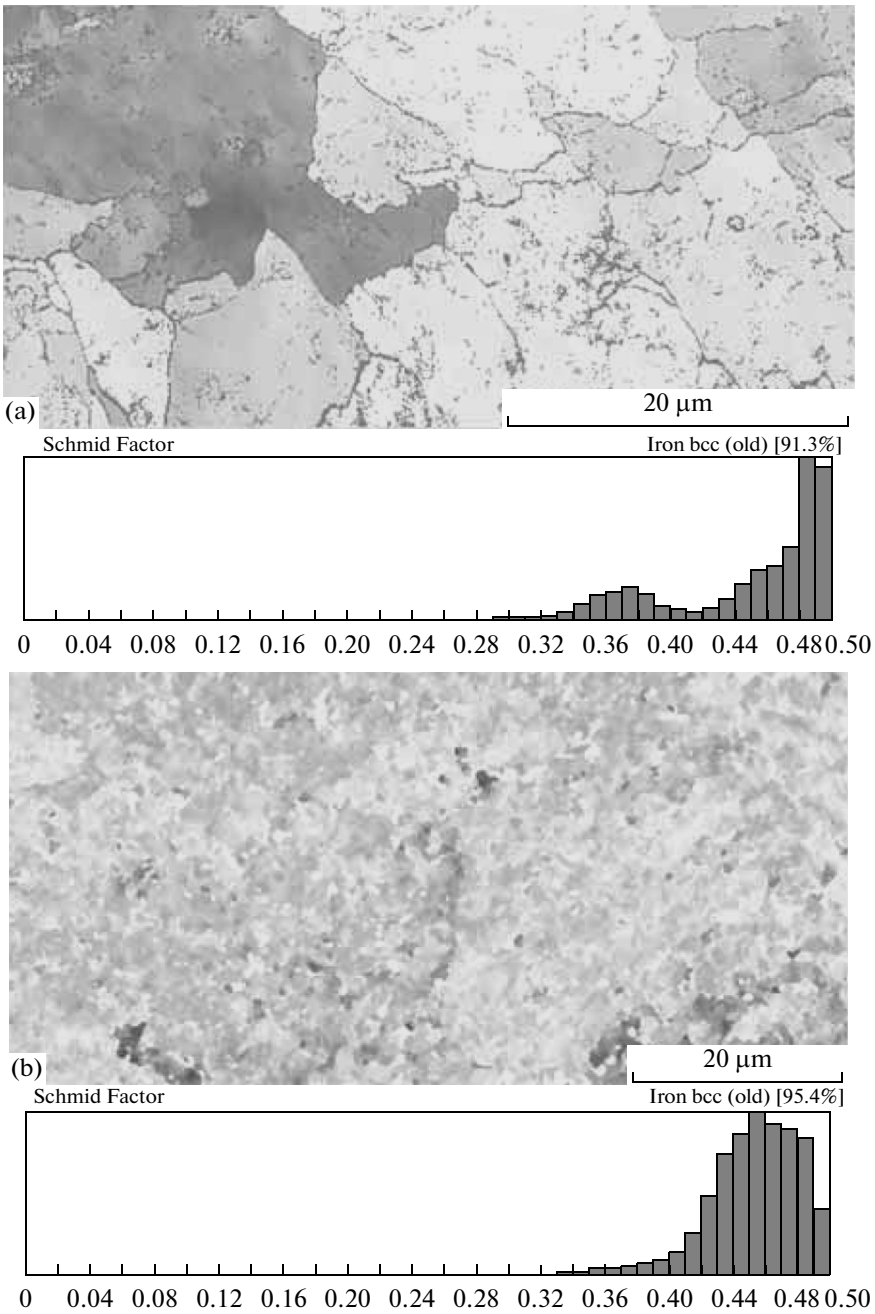

Fig. 8. The Schmidt factor map for (a) coarse and (b) fine crystallites. {101}⟨111⟩ deformation system, the loading direction is parallel to the *OX* axis. Bright areas correspond to higher values of the Schmidt factor. Under an external load, deformations will start to occur in bright grains and gradually propagate to dark grains.

ning electron microscopy using X-ray spectral microanalysis and electron backscatter diffraction. Element distribution maps for the inclusion zone were plotted (Figs. 5a–5c). Specimens that were taken from the roll defect zone in accordance with ultrasonic inspection data were examined. Qualitative metallographic analysis revealed three types of defects whose sizes are substantially smaller than those identified by ultrasonic inspection means. The characteristic size of inclusions from the first group was about 1 μm; these inclusions contained Si, O, and Al (Fig. 5a). Some of them contained globular regions enriched with carbon. These inclusions result from the entry of a refractory material into a fluid metal or agglomerates of deoxidizing products. Figure 5b shows the element distribution map for the second type of inclusions. The inclusions of the second type are spherically shaped and have a characteristic size of about 5 μm; these inclusions are uniformly distributed over the entire surface of the section. They are characterized by

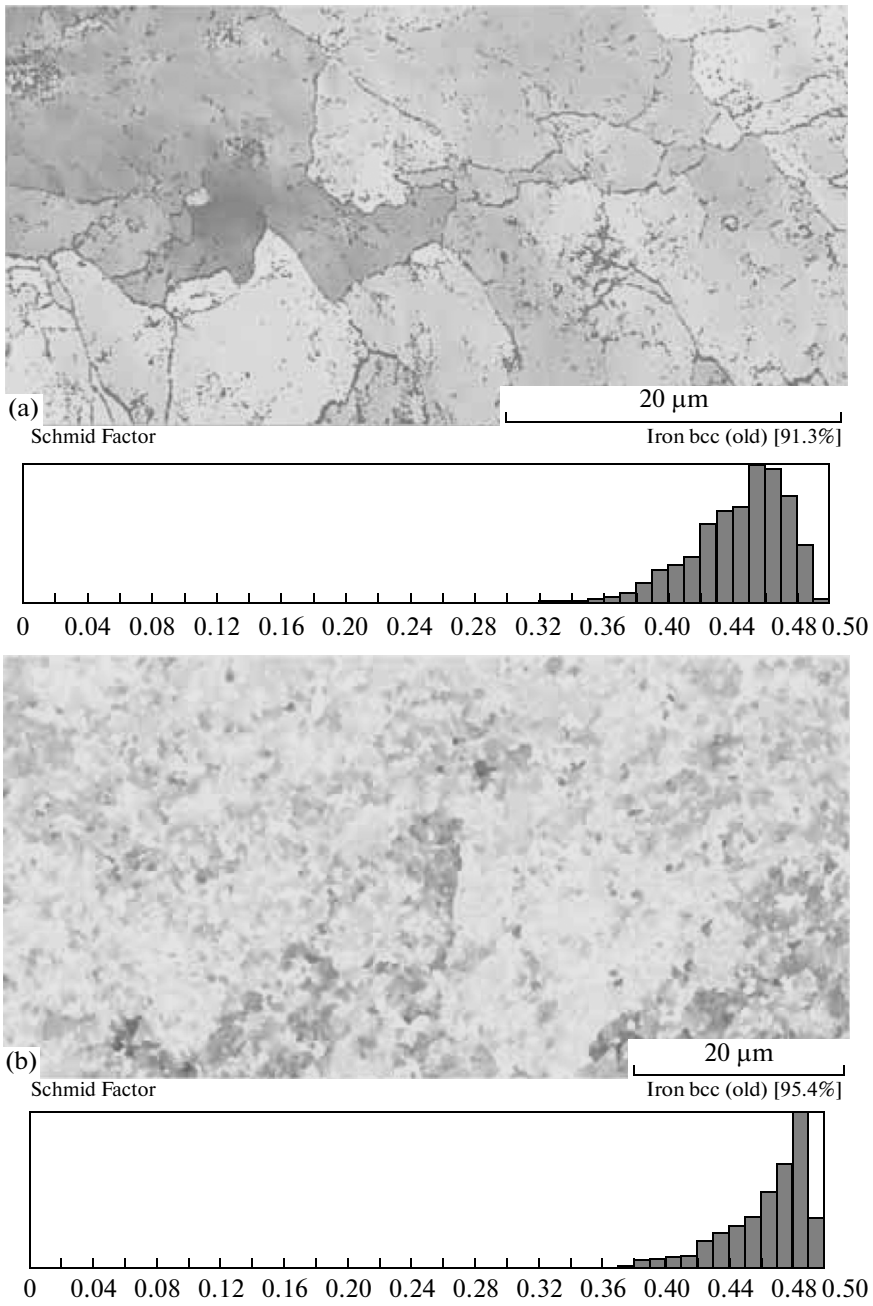

Fig. 9. The Schmidt factor map for (a) coarse and (b) fine crystallites. {211}⟨111⟩ deformation system, the loading direction is parallel to the *OX* axis. Bright areas correspond to higher values of the Schmidt factor. Under an external load, deformations will start to occur in bright grains and gradually propagate to dark grains.

increased concentrations of Si and O, which is indicative of their origin, i.e., they are particles of refractory materials. Inclusions of the third type are the largest; they have a complex structure and a characteristic size of about 20 μm (Fig. 5c). The inclusions of the third type contain particles that are rich in Si and O in a surrounding that is rich in S and Mn [5]. These inclusions can result from the presence of low-melting Fe–FeO–FeS eutectic that is located along grain boundaries due to the presence of an excess amount of oxygen and sulfur in the metal. It is known that oxygen reduces the melting temperature of Fe–FeO–FeS eutectic [5]. Nonmetal inclusions whose elastic characteristics differ from those of steel cause the scattering of ultrasonic waves. As was noted in [7], scattering depends on the ratio between the wavelength and the size of a microdefect. It was shown by I.M. Lifshits and G.D. Parkhomovskii [8] that, at $\lambda/d \sim 800$

(small inclusions) and $\lambda/d \sim 80$ (large inclusions), the absorption coefficient is proportional to the frequency to the fourth power ($\lambda > d$).

The metallographic study of specimens of the 9X2MΦ steel taken from the defect zone using electron backscatter diffraction has shown that they have a polycrystalline structure. Figure 6 shows crystallite orientation maps (Euler angles). Areas with coarse-crystalline and fine-crystalline structures are found with a characteristic crystallite size of 10 and 1 μm, respectively (Figs. 6a and 6b). Misorientation histograms for coarse and fine crystallites are plotted (Figs. 7a and 7b). Correlated misorientations correspond to these orientations between the neighbor points and uncorrelated misorientations correspond to these orientations between the points randomly selected from a data set. The theoretical curve shows the expected result for a random data set. It can be seen that the correlated (blue) and uncorrelated (red) misorientations substantially differ from the theoretical curve and from each other. The difference between the uncorrelated misorientations and the theoretical curve is mainly due to pronounced texture. The correlated distribution histogram for fine crystallites shows a large number of low-angle boundaries, i.e., boundaries with a misorientation angle of less than 15 deg that are not seen in the uncorrelated distributions. The analysis of the misorientation angle histograms for coarse and fine crystallites shows that, in the first case, a large number of high-angle boundaries are found and, in the second case, a less pronounced texture of the material occurs. In both cases, the metal is textured, which must affect its acoustic characteristics [7].

The results of the analysis of Kikuchi diffraction patterns allowed us to plot Schmidt factor maps for deformation systems that are typical of αFe, i.e., $\{101\}\langle 111\rangle$ and $\{211\}\langle 111\rangle$ when the loading direction is parallel to the *OX*-axis. The Schmidt factor maps for the $\{101\}\langle 111\rangle$ and $\{211\}\langle 111\rangle$ deformation systems when the loading direction is parallel to the *OX*-axisare presented in Figs. 8 and 9, respectively. The following notation for the Schmidt factor maps is used: bright areas correspond to higher values of the Schmidt factor. Under an external load, deformations will start to occur in bright grains and gradually propagate to dark grains. It is known that the applied mechanical stress σ and the shear stress in the slip system τ are related as follows: $\tau = m\sigma$, where $m = \cos\lambda \cos\chi$ is the Schmidt factor or the orientation factor; λ is the angle between the slip direction and the deformation axis; and χ is the angle between the normal to the slip plane and the deformation angle. The maximum value of the Schmidt factor is apparently 0.5 at $\lambda = \chi = \pi/4$. We note that for coarse crystallites the Schmidt factor histogram or the orientation factor diagram for the $\{101\}\langle 111\rangle$ deformation system has two maxima (Fig. 8), which is indicative of the nonuniformity of the elastic characteristics, including the acoustic characteristics.

It is known [7] that in the majority of cases the attenuation of ultrasound in polycrystalline materials is related to scattering on grains, which leads to the loss of the energy of a propagating wave. The scattering is due to a difference in the modulus and density of the boundary from those of the grain core, i.e., the grain boundary is a discontinuity flaw. E. Papadakis noted that the attenuation of ultrasonic waves during inspection is affected by the size distribution of grains and their predominant orientation, as well as the fact that the grains are nonequiaxed and contain several phases [7]. These factors should be allowed for during the ultrasonic quality inspection of steel articles that have a polycrystalline structure.

CONCLUSIONS

The microstructure of specimens of 9X2MΦ steel that was taken from ready-made working rolls of a mill was examined. These specimens were taken from the zone of the agglomeration of discontinuity flaws with a reflection power equivalent to ∅2–4 mm; in places, no bottom signal was recorded. The metallographic analysis of the specimens was carried out by means of traditional methods implemented using a scanning electron microscope; X-ray spectral microanalysis and electron backscatter diffraction were used. The morphology and elemental composition of discontinuity flaws were studied, as well as phase maps, crystallite misorientation histograms, and Taylor factor maps were plotted for specimens taken from the defect zone of a working roll. A correlation between the characteristics of the crystal structure of the metal and the intensified attenuation of ultrasonic waves was found. In particular, three types of defects were found in the defect zone, whose size was substantially less than that identified by ultrasonic inspection means, i.e., from 1 to 20 μm. Small (about 1 μm in size) inclusions result from the entry of a refractory material into a fluid metal or the agglomeration of deoxidizing products; large (about 20 μm in size) inclusions, from the presence of low-melting Fe–FeO–FeS eutectic that is located along grain boundaries due to the presence of an excess amount of oxygen and sulfur in the metal. Zones with coarse-grained and fine-grained structures are found; the characteristic crystallite size is 10 and 1 μm, respectively. Fine crystallites have low-angle boundaries, i.e., boundaries with a misorientation angle of less than 15 deg; coarse crystallites have a large number of high-angle boundaries. In both cases, the metal is textured, which must

affect its acoustic characteristics [7]. We note that, for coarse crystallites, the Schmidt factor histogram for the $\{101\}\langle 111\rangle$ deformation system has two maxima, which is indicative of the nonuniformity of the elastic characteristics, including the acoustic characteristics.

Thus, it is found that the attenuation of ultrasonic waves during inspection when no bottom signal is recorded is due to both nonmetal inclusions and to various grain sizes, as well as the predominant orientation of the grains and the fact that the grains are nonequiaxed. These factors should be allowed for during the ultrasonic quality inspection of steel articles that have a polycrystalline structure; their contribution to the result will be investigated in our future works.

REFERENCES

1. Kretov, E.F., *Ul'trazvukovaya defektoskopiya v energomashinostroenii* (Ultrasonic Inspection in Power Machine Building), St. Petersburg: Radioavionika, 1995.
2. Murav'ev, V.V., Zuev, L.B., and Komarov, K.L., *Skorost' zvuka i struktura stalei i splavov* (Sound Speed and Structure of Steels and Alloys), Novosibirsk: Nauka, Sibirskaya izdatel'skaya firma RAN, 1996.
3. Vybornov, B.I., *Ul'trazvukovaya defektoskopiya* (Ultrasonic Inspection), Moscow: Metallurgiya, 1985.
4. Aleshin, N.P., Belyi, V.E., Vopilkin, A.Kh., et al., *Metody akusticheskogo kontrolya metallov* (Methods for Acoustic Inspection of Metals), Aleshin, N.P, Ed., Moscow: Mashinostroenie, 1989.
5. *Atlas defektov stali* (Steel Defect Atlas), German Translation, Moscow: Metallurgiya, 1979.
6. *Metallografiya zheleza* (Metallography of Iron), German Translation, Lyamber N., Gredi T., Khabraken L., et al., Eds., Moscow: Metallurgiya, 1985.
7. *Primenenie fizicheskoi akustiki v kvantovoi fizike i fizike tverdogo tela* (Application of Physical Acoustics in Quantum Physics and Physics of Solids), Mason, U, Ed., Moscow: Mir, 1970.
8. Lifshits, I.M. and Parkhomovskii, G.D., On theory of propagation of ultrasonic waves in polycrystals, *Zh. Eksp. Teor. Fiz.*, 1950, vol. 20, no. 2, pp. 175–182.

Translated by D. Tkachuk